Tuning the porosity and photocatalytic performance of triazine-based graphdiyene polymers *via* polymorphism

Dana Schwarz,[a] Amitava Acharjya,[b] Arun Ichangi,[a],[c] Yaroslav S. Kochergin,[a] Pengbo Lyu,[d] Maksym V. Opanasenko,[d, e] Ján Tarábek,[c] Jana Vacek Chocholoušová,[c] Jaroslav Vacek,[c] Johannes Schmidt,[b] Jiří Čejka,[d, e] Petr Nachtigall,[d] Arne Thomas[b] and Michael J. Bojdys*[a, c]

Abstract: Crystalline and amorphous organic materials are an emergent class of heterogeneous photocatalysts for the generation of hydrogen from water, but a direct correlation between their structures and the resulting properties has not been achieved so far. To make a meaningful comparison between structurally different, yet chemically similar porous polymers, we present two porous polymorphs of a triazine-based graphdiyene (TzG) framework from a simple, one-pot reaction using Cu(I) for TzG_{Cu} and Pd(II)/Cu(I) for $TzG_{Pd/Cu}$ catalyzed homocoupling polymerization. The polymers form *via* irreversible coupling reactions and give rise to a crystalline (TzG_{Cu}) and an amorphous ($TzG_{Pd/Cu}$) polymorph. Notably, the crystalline and amorphous polymorphs are narrow-gap semiconductors with permanent surface areas of 660 m^2 g^{-1} and 392 m^2 g^{-1}, respectively. Hence, both polymers are ideal heterogeneous photocatalysts for water splitting with some of the highest hydrogen evolution rates reported thus far up to 972 µmol h^{-1} g^{-1} with and 276 µmol h^{-1} g^{-1} without Pt co-catalyst. We conclude, that crystalline order improves delocalisation, while the amorphous polymorph requires a co-catalyst for efficient charge transfer; this will need to be considered in future rational design of polymer catalysts and organic electronics.

Organic porous polymer networks have recently attracted considerable attention as gas storage materials and as heterogeneous catalysts, particularly in photocatalytic hydrogen evolution.[1] The introduction of heteroatoms such as nitrogen into organic polymers has led to the discovery of organic semiconductors,[2] metal-free catalysts for hydrogen evolution from water,[3] or catalysts for CO_2 fixation.[4] In addition, (C, N)-containing crystalline frameworks are candidate materials for "postsilicon electronics".[5] Two major classes of organic porous polymers emerged over the last 15 years, based on two distinct design principles. On the one hand, covalent organic frameworks (COFs) feature a predictable, long-range order of building blocks. These COFs are linked by covalent, yet reversible, bond formation.[6] On the other hand, conjugated microporous polymers (CMPs) have enhanced stability and optical properties thanks to overall π-conjugation between building blocks, albeit at the expense of structural order.[7] These systems are of great interest not only because they have the potential to combine high surface areas with useful (opto-)electronic effects, but also because they offer – in principle – a wide scope for the rational design of their structures and properties. However, a direct comparison of the structure-properties relationship between ordered COFs and amorphous CMPs has not been possible so far because the underlying chemistry of their respective building blocks and their linking chemistry is fundamentally different.
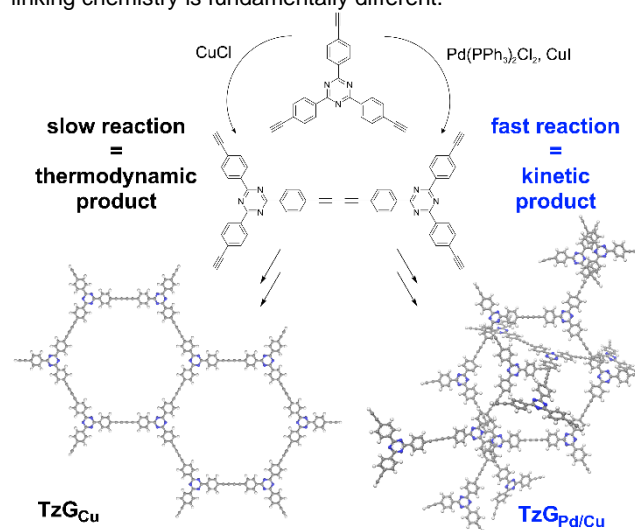
Figure 1. Reaction scheme for the formation of the thermodynamic, ordered TzG_{Cu} (left, black) and the kinetic, disordered $TzG_{Pd/Cu}$ (right, blue) polymorphs starting with the synthon (2,4,6-tris(4-ethynylphenyl)-1,3,5-triazine). Both reactions yield the buta-1,3-diyne bridged products.

[a]   Dr. D. Schwarz, Y. S. Kochergin, A. Ichangi, Dr. M. J. Bojdys
        Faculty of Science, Department of Organic Chemistry
        Charles University
        Hlavova 8, 128 43 Prague 2, Czech Republic
        E-mail: m.j.bojdys.02@cantab.net
[b]   A. Acharjya, Dr. J. Schmidt, Prof. Dr. Arne Thomas
        Institute of Chemistry
        Technische Universität Berlin
        Hardenbergstraße 40, 10623 Berlin, Germany
[c]   A. Ichangi, Dr. J. Tarábek, Dr. J. Vacek Chocholoušová, Dr. J. Vacek, Dr. M. J. Bojdys
        Institute of Organic Chemistry and Biochemistry of the CAS, Flemingovo nám. 2, 166 10 Prague 6, Czech Republic
[d]   Dr. M. V. Opanasenko, Prof. Dr. J. Čejka, P. Lyu, Prof. Dr. P. Nachtigall,
        Faculty of Science, Department of Physical and Macromolecular Chemistry
        Charles University
        Hlavova 8, 128 43 Prague 2, Czech Republic
[e]   Dr. M. V. Opanasenko, Prof. Dr. J. Čejka
        J. Heyrovský Institute of Physical Chemistry of the CAS, v.v.i.
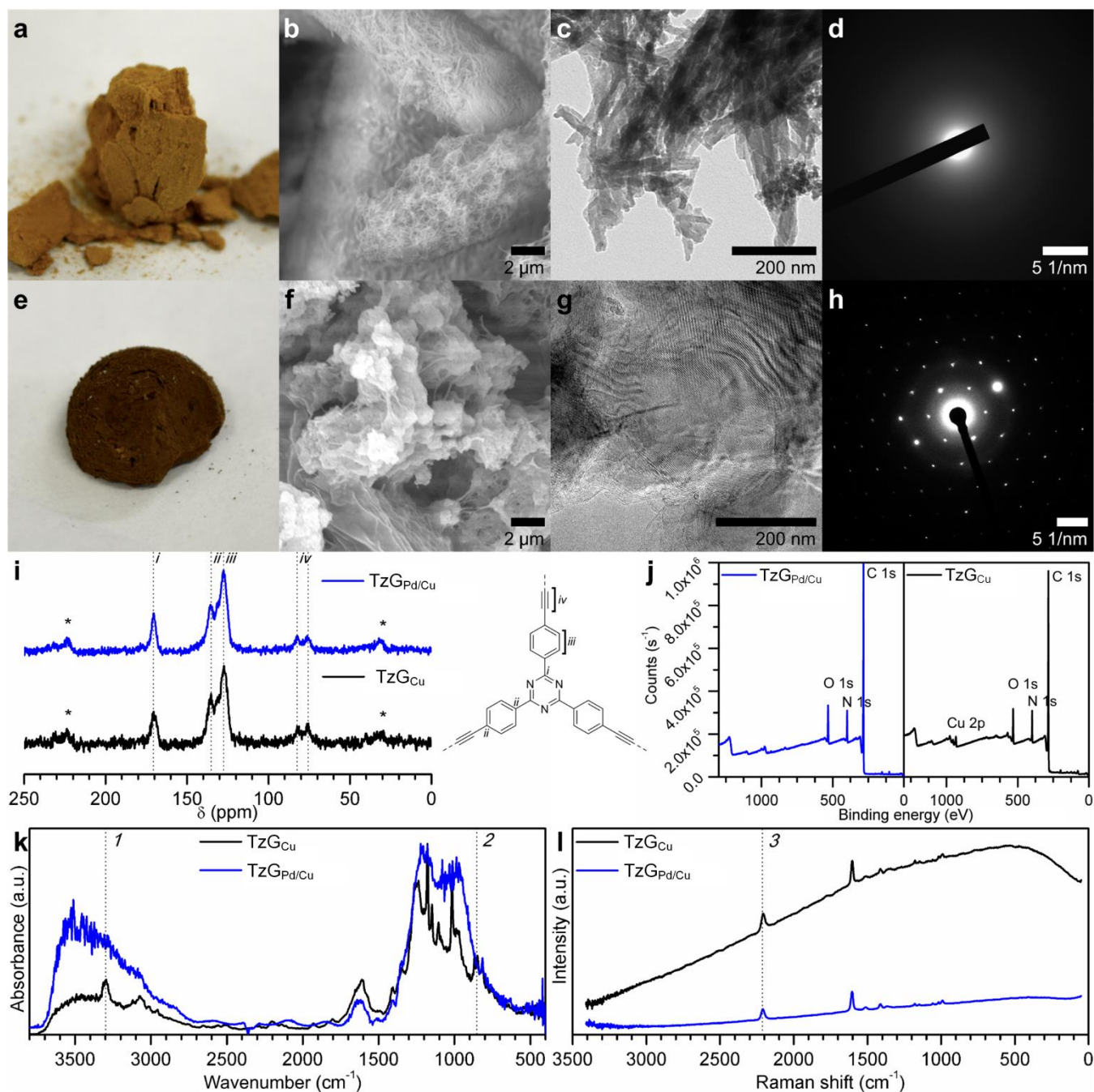   Dolejškova 2155/3, 182 23 Prague 8, Czech Republic

        Supporting information for this article is given via a link at the end of the document.

In this study, we address the importance of the structural order of organic porous polymers for the (opto-)electronic

Figure 2. Composition and morphology of TzG polymers obtained *via* a coupling reaction with CuCl or Pd(PPh₃)₂Cl₂/CuI as catalyst. Photographs of a) TzG$_{Pd/Cu}$ and e) TzG$_{Cu}$ as-synthesised powders. SEM images show aggregated strands for b) TzG$_{Pd/Cu}$ and overgrown layers for f) TzG$_{Cu}$. TEM images of c) TzG$_{Pd/Cu}$ show rod-like structures with diameters of 20 nm and no discernible internal structure, whereas g) TzG$_{Cu}$ features highly-crystalline sheets on the order of 500-1000 nm. Corresponding electron diffraction images confirm that d) TzG$_{Pd/Cu}$ has no internal crystallinity, whereas h) TzG$_{Cu}$ shows pronounced hexagonal diffraction spots. i) ¹³C CP-MAS NMR of TzG$_{Pd/Cu}$ (blue) and TzG$_{Cu}$ (black). The triazine carbon signal (marked *i*) appears at 170 ppm, and the quaternary diyene carbons (marked *iv*) at around 80 ppm. Phenyl peaks are marked as *ii* and *iii*. Spinning side bands are denoted with an asterisk (*). j) XPS data for TzG$_{Pd/Cu}$ (left, blue) and TzG$_{Cu}$ (right, black) shows near identical plots and composition, except for some residual copper in TzG$_{Cu}$. k) FT-IR spectra of TzG$_{Pd/Cu}$ (blue) and TzG$_{Cu}$ (black). Terminal unreacted C≡C–H bonds are identified as *1*, while the characteristic triazine breathing mode is observed at *2*. l) Raman spectra of TzG$_{Pd/Cu}$ (blue) and TzG$_{Cu}$ (black) at 780 nm. The characteristic diyene stretch can be discerned for both polymers at ~ 2200 cm⁻¹ (marked as *3*).

properties of the bulk materials. For this purpose, we use a modular, synthetic platform of triazine-based graphdiyne (TzG) that enables the synthesis of ordered and amorphous networks while maintaining desirable π-conjugation (Figure 1). Triazine-

based graphdiyne features an intriguing donor–acceptor (D–A) motif consisting of electron-rich buta-1,3-diyene (D) and electron-poor triazines (A). Indeed, the triazine (C_3N_3, Tz) core is predicted to offer larger hyperpolarisabilities than the analogous carbon-

only benzene core because triazine is more electron withdrawing and nucleophilic.[8] Triazine is a particularly interesting structural motif for the design of organic polymer networks because it combines heteroatoms held in π-conjugation and C_3 symmetric co-planarity.[9] We have successfully used this D–A motif of TzG as part of a 2D/3D van der Waals heterostructure for (noble metal-free) photocatalytic hydrogen evolution.[10]

Triazine-based graphdiyene polymers are constructed using the principle synthon 2,4,6-tris(4-ethynylphenyl)-1,3,5-triazine that consists of a central 1,3,5-triazine moiety connected to 1,4-phenyl rings and is terminated by ethynes. Details of the synthesis are found in the Supporting Information (Scheme S1). In brief, the triazine ring was formed by treating 4-bromobenzonitrile with trifluoromethanesulfonic acid.[11] The trimethylsilyl group protected acetylene group was attached to the molecule by Negishi coupling. Deprotection occurs in a good yield by adding K_2CO_3 in THF/MeOH. The triazine-based graphdiyne polymer (TzG) was obtained using CuCl (TzG_{Cu}) or Pd(PPh$_3$)$_2$Cl$_2$ with CuI ($TzG_{Pd/Cu}$) as catalysts (Figure 1). The network-forming reaction that couples ethynes into 1,3-diyne bridges is commonly achieved by Glaser coupling using a copper(I) salt.[12] Alternatively, the diacetylene bridge can be formed under common and efficient Sonogashira-like conditions.[13] Numerous studies show that combined catalytic systems – for example, Pd(0) or Pd(II) together with Cu(I) – couple terminal acetylenes faster and at higher yields than traditional Glaser protocols that use Cu(I) salts only.[14] While highly efficient coupling is beneficial for small molecule synthesis, we believe that it can lead to the preferred formation of kinetic and disordered rather than thermodynamic and ordered materials.

Either reaction pathway yields buta-1,3-diyne bridged TzG polymers (Figure 2i, k, l). We confirm the chemical composition of TzG by ICP-OES (see Supporting Information) and ^{13}C cross-polarisation magic angle spinning (CP-MAS) solid-state NMR (Figure 2i). Both polymers match the theoretical, stoichiometric C/N ratio of 9:1 (Table S1 and S2) and feature the triazine carbon (~170 ppm) and the diyene (~80 ppm) signals. Fourier-transform infrared spectroscopy (FT-IR) (Figure 2k, Figure S1) shows characteristic signals at 3290 cm^{-1} corresponding to C≡C, and strong peaks at 1359 cm^{-1} and 816 cm^{-1} ascribed to the breathing modes of the triazine ring.[15] The peaks at 2200 cm^{-1} and 1929 cm^{-1} correspond to the buta-1,3-diyne bridge (-C≡C-C≡C-).[16] The sluggish Glaser reaction gives rise to a few unreacted C≡C-H end-groups at 3300 cm^{-1}. These end-groups, however, are not discernible in ^{13}C CP-MAS NMR (c.f. Figure 2i), hence, they are most likely only found at the external surfaces of TzG_{Cu} particles and do not dominate the bulk. Raman spectra of TzG_{Cu} and $TzG_{Pd/Cu}$ show C≡C stretching at ~2200 cm^{-1} (Figure 2l). X-ray photoelectron spectroscopy (XPS) shows that TzG_{Cu} retains some copper catalyst – 0.85 wt% by EDX (Table S1) and up to 4.45 wt% by inductively coupled plasma optical emission spectrometry (ICP-OES) (Table S2), thermogravimetric analysis (TGA) (Figure S2), and– either as Cu metal, or Cu(I) oxides (Figure 2j, Figure S3). The difference in copper content from both methods indicates that copper is embedded within the polymer matrix away from the external surfaces, and that it is unlikely to affect the photocatalytic activity and bulk properties of the polymer at such low quantities, as previously shown.[10]

As expected, we see no long range order for the polymer obtained via a Sonogashira-like coupling (Figure 2d),[17] and it is likely that interdigitation of polymer strands and rings occurs because pore sizes are sufficiently large (Figure 2d, Figure 3c).[18] In contrast, TzG_{Cu} has a high degree of crystalline order. Small-angle X-ray scattering (SAXS) shows a diagnostic, low-angle peak that is absent for $TzG_{Pd/Cu}$ (Figure 3c, Figure S5). This feature corresponds to the (100) reflection of a hexagonal unit cell with 2D lattice parameters $a = b = 30.7898$ Å (Figure 3d). We use density functional theory (DFT) calculations to predict feasible packing arrangements of TzG_{Cu} layers (see Supporting Information). Turbostratic stacking disorder and low energy gains from different stacking modes are known for analogous, π-stacked systems.[19] Here, we compare DFT results against physical data from high-resolution transmission electron microscopy (HR-TEM, Figure 3a, Figure S6) and selected area electron diffraction (SAED, Figure 3b, Figure S6). The best fit is achieved using a DFT optimised, ABC-stacked TzG_{Cu} structure with a unit-cell of $a = b = 30.7898$ Å, $c = 6.1397$ Å, and space group R-3M (no. 166) (Figure 3d, and e, Figure S8).
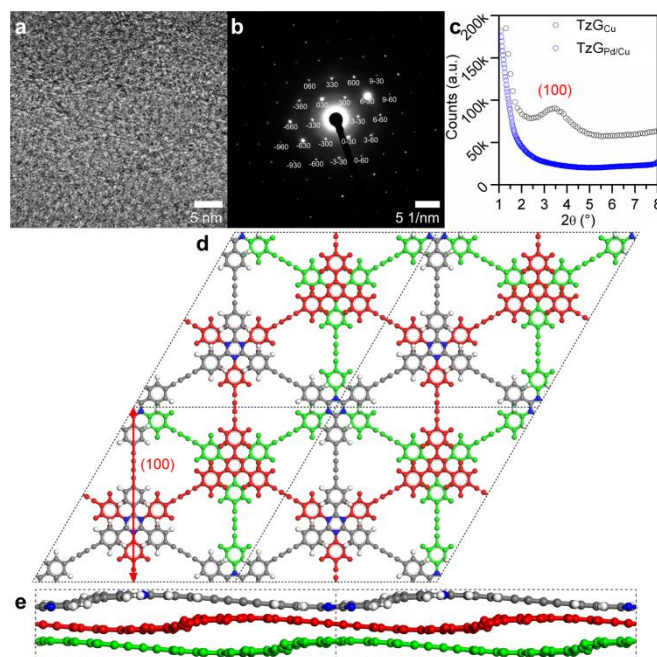

Figure 3. Structure analysis of the crystalline TzG_{Cu} polymorph. a) The high-resolution TEM image of TzG_{Cu} reveals a hexagonal bonding motif, and b) the selected area electron diffraction pattern corresponds to a covalently bonded, ABC-stacked TzG structure. c) The small-angle X-ray diffraction pattern of TzG_{Cu} (black) shows a characteristic (100) peak that is absent in $TzG_{Pd/Cu}$ (blue). The ABC packing motif of TzG_{Cu} (with the lower-lying layer indicated in red and green) is shown along the c-vector in d) and along the ab-vector in e). This is a stable structure obtained at DFT level with unit cell parameters of $a = b = 30.7898$ Å, $c = 6.1397$ Å, space group R-3M (no. 166). The characteristic (100) repeat is marked in red.

UV/Vis spectra of TzG_{Cu} and $TzG_{Pd/Cu}$ polymorphs have a similar absorption edge at ~580 nm, yet the spectrum of TzG_{Cu} shows a long tail towards the visible region (Figure 4a). This feature is a direct effect of the improved planarity of crystalline TzG_{Cu} and is thought to be caused by exciton-hopping between

layers.[20] Consequently, TzG$_{Cu}$ appears darker (*c.f.* Figure 2e) and the the Kubelka-Munk function predicts a direct optical band gap of 2.04 eV and an indirect optical band gap of 0.88 eV (Figure 4c). TzG$_{Pd/Cu}$ has a direct optical band gap of 1.97 eV and an indirect optical band gap of 1.23 eV, according to the same calculation (Figure 4b). The colour of a material – and, hence, the derived optical band gap – is a bulk effect of layer stacking (or lack thereof). Therefore, colour can be misleading when analysing the actual electronic band gap, in particular when the volume, mass and density of the UV/Vis irradiated material are unknown.[21] Hence, we complement the investigation of optical properties of both polymorphs by photoluminescence (PL) spectroscopy. Both materials show near-identical excitation spectra with peak maxima centred at ~480 nm corresponding to exciton transition energies of 2.5 - 2.6 eV (Figure 4d). The lack of structural order of the TzG$_{Pd/Cu}$ polymorph inhibits exciton annihilation, which often occurs in tightly packed, π-aromatic systems.[11, 22] Consequently, the PL response of TzG$_{Pd/Cu}$ in excitation and emission is one to two orders of magnitude higher than that of TzG$_{Cu}$ (Figure 4d and e). DFT calculations (using the PBE0 hybrid functional with many body dispersion in the FHI-Aims code) predict that the overall HOMO-LUMO gap of a TzG

material is 2.60 eV which appears to be an indirect band gap. The smallest direct gap is 2.93 eV (Figure 4f – h, Figure S8). Hence, both TzG polymorphs are expected to be indirect band gap semiconductors.

In order to clarify how polymorphisms affect the spin states, we examine both polymorphs by electron paramagnetic resonance (EPR). Both TzG$_{Cu}$ and TzG$_{Pd/Cu}$ are EPR active and display an intense polaronic-like spectrum at similar *g* values of 2.0032 (linewidth 0.63 mT) and 2.0035 (linewidth 0.66 mT), respectively (Figure 4i). This is comparable to other conductive polymers (*g* values of 2.0030-2.0035, and linewidths of 0.42-0.80 mT).[23] Note though, that the radical component of TzG$_{Cu}$ has a two-fold higher intensity (Figure 4i). This indicates a higher concentration of induced polaron-like centres in TzG$_{Cu}$ than in TzG$_{Pd/Cu}$ – presumably caused by denser, crystalline packing. There is no qualitative difference between the spin delocalisation along the π-aromatic backbone of both polymorphs, as observed previously for compounds with π-aromatic domains of varying sizes.[24] Hence, the observed optical differences between the two polymorphs are purely a morphological effect.
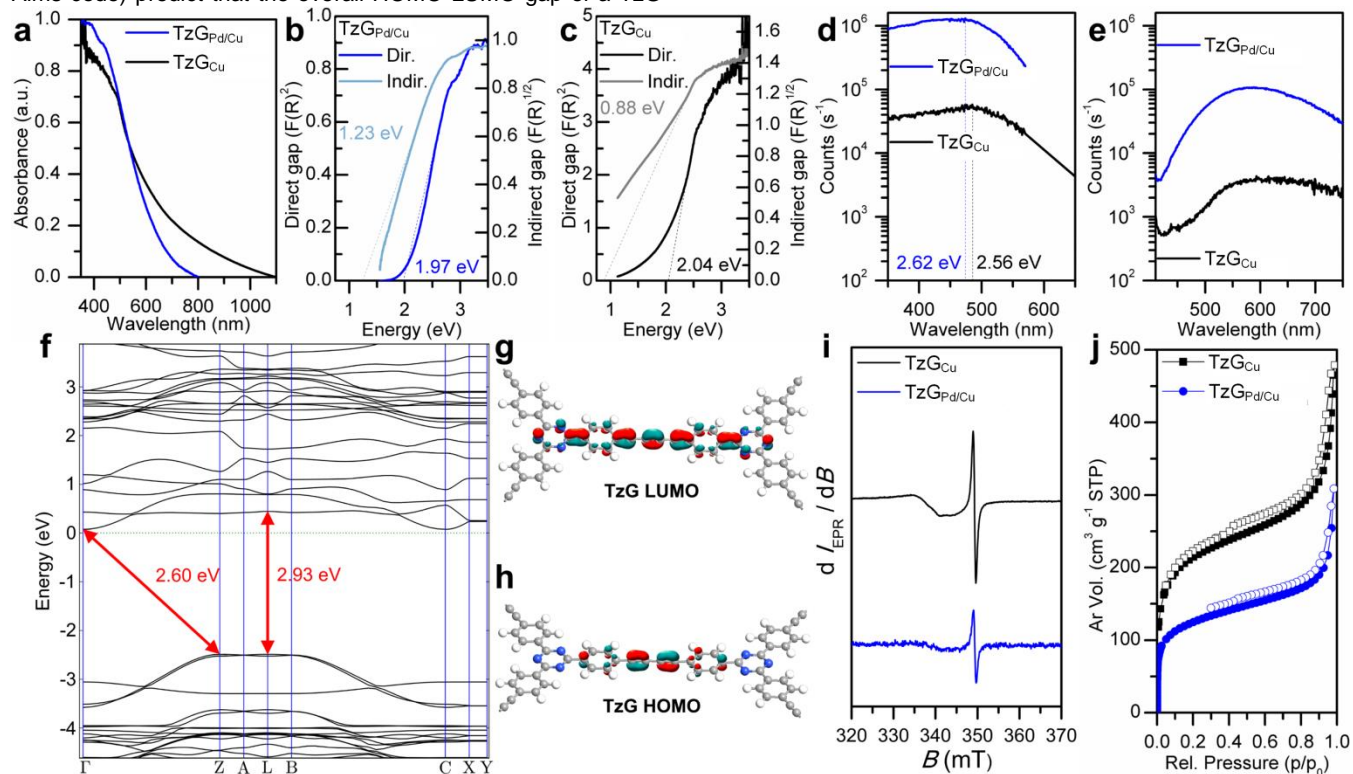

Figure 4. Optical, electronic and sorption properties of TzG$_{Pd/Cu}$ and TzG$_{Cu}$ polymorphs. a) Solid-state UV/Vis diffuse-reflectance spectrum of TzG$_{Pd/Cu}$ (blue) and TzG$_{Cu}$ (black), and the corresponding Kubelka-Munk plots for b) TzG$_{Pd/Cu}$ with a direct (1.97 eV) and indirect (1.23 eV) optical band gap, and for c) TzG$_{Cu}$ with a direct (2.04 eV) and indirect (0.88 eV) optical band gap. d) Photoluminescence emission and e) excitation spectra for TzG$_{Pd/Cu}$ (blue) and TzG$_{Cu}$ (black). The two maxima at 2.62 eV and 2.56 eV are attributed to excitation transitions within TzG$_{Pd/Cu}$ and TzG$_{Cu}$, respectively. f) The band gap diagram for TzG indicates an indirect band gap of 2.60 eV and a direct band gap of 2.93 eV. g and h) Plots of orbital coefficients for the frontier orbitals of TzG as derived from DFT calculations. i) Experimental EPR spectrum of TzG$_{Pd/Cu}$ (blue) and TzG$_{Cu}$ (black). The radical component of TzG$_{Cu}$ (*g* factor 2.0032, linewidth 0.63 mT) is two-times more intense than that of TzG$_{Pd/Cu}$ (*g* factor 2.0035, linewidth 0.66 mT), indicating a higher concentration of induced polaron-like centres in TzG$_{Cu}$ than in TzG$_{Pd/Cu}$. The spectrum of TzG$_{Cu}$ shows in addition a feature between 340 mT and 345 mT that corresponds to paramagnetic Cu^{2+} species.[10] j) Argon sorption isotherms for TzG$_{Pd/Cu}$ (blue) and TzG$_{Cu}$ (black) measured at 87 K.

The pore structure of both polymorphs was investigated by argon sorption (Figure 4j, Table S4). The TzG_{Cu} polymorph has a higher specific surface area (660 m^2 g^{-1}) than $TzG_{Pd/Cu}$ (392 m^2 g^{-1}), according to the Brunauer-Emmett-Teller (BET) model. The dominant micropore size diameter for both polymorphs is ~0.6 nm, which was calculated using the BJH model (Figure S10). The adsorption and desorption branches for both polymorphs show no discernible hysteresis over the mesoporous and microporous range. Hence, we can assume that both polymorphs have similar rigidity with little or no swelling. Consequently, the comparatively smaller accessible surface area of $TzG_{Pd/Cu}$ is presumably not a consequence of pore collapse but more likely, a result of pore blockage *via* interdigitation (or inter-growth) during its kinetically controlled formation. The relatively small micropores in both materials are ideal for CO_2 uptake with high values of 2.23 mmol g^{-1} for $TzG_{Pd/Cu}$ and 2.02 mmol g^{-1} for TzG_{Cu} at 273 K (Figure S11).

Evidently, both TzG polymorphs combine a useful band gap and permanent pore structure; hence, they are interesting candidates as heterogeneous photocatalysts in light-promoted hydrogen evolution from water. We perform the hydrogen evolution experiments by irradiating a suspension of TzG powders in a water:acetonitrile mixture (1:1) at room temperature with visible light (395 nm cut-off filter). Triethanolamine (TEOA) is the sacrificial electron donor, and the reaction is performed with and without platinum (Pt) co-catalyst (see Supporting Information).[2] The disordered $TzG_{Pd/Cu}$ polymorph shows one of the highest hydrogen evolution rates reported for this class of polymeric materials (972 μmol h^{-1} g^{-1} and 101 μmol h^{-1} g^{-1} without Pt), comparable to CTF-1 – a covalent triazine framework (1072 μmol h^{-1} g^{-1}).[25] TzG_{Cu} performs at 490 μmol h^{-1} g^{-1} (276 μmol h^{-1} g^{-1} without Pt). Interestingly, the co-catalyst has the strongest effect on the photocatalytic performance $TzG_{Pd/Cu}$ – the disordered material with no inter-plane annihilation pathways for generated excitons as shown by UV/Vis. Indeed, Pt usually mediates the transfer of electrons from the photoactive framework to the sites of water reduction;[26] which is not efficiently achieved by $TzG_{Pd/Cu}$ alone. The addition of Pt has a markedly lower effect on TzG_{Cu}. Here, improved inter-layer packing leads to a relatively efficient electron transfer, with or without a co-catalyst, as shown previously for crystalline, conductive triazine films.[10]

In summary, we demonstrate a direct correlation between structure and properties, such as crystallinity vs. disorder and its impact on charge carrier mobility and catalytic activity. We study the photocatalytic hydrogen evolution rates of amorphous $TzG_{Pd/Cu}$ and crystalline TzG_{Cu} using sacrificial hole-scavengers and compare the performance and (opto-)electronic properties of the materials with predictions of DFT calculations and evidence from spectroscopic and crystallographic measurements. The ordered TzG_{Cu} polymorph has the highest accessible surface area and a co-planar π-conjugated backbone that yields itself to inter-plane hopping of charge carriers and a more efficient electron transfer. In contrast, the disordered $TzG_{Pd/Cu}$ polymorph shows inter-growth, pore blockage and isolated π-aromatic segments. This lack of pathways for exciton annihilation give rise to a highly fluorescent material that – in terms of photocatalytic performance – benefits most from a noble metal co-catalyst that mediates electron transfer. More importantly, for the first time, we combine the worlds of ordered, covalent organic frameworks and disordered, conjugated microporous polymers in a comprehensive polymorph study based on the highly modular and malleable synthetic platform of triazine-based graphdiyene polymers. This lays the foundations for truly rational design of functional nanomaterials – be it as tailored upconverting phosphors, heterogeneous catalysts or in (opto-)electronic applications.

[1]   aJ. X. Jiang, Y. Y. Li, X. F. Wu, J. L. Xiao, D. J. Adams, A. I. Cooper, *Macromolecules* **2013**, *46*, 8779-8783; bJ. X. Jiang, A. Trewin, D. J. Adams, A. I. Cooper, *Chem. Sci.* **2011**, *2*, 1777-1781; cG. G. Zhang, Z. A. Lan, X. C. Wang, *Angew. Chem., Int. Ed.* **2016**, *55*, 15712-15727; dR. S. Sprick, B. Bonillo, R. Clowes, P. Guiglion, N. J. Brownbill, B. J. Slater, F. Blanc, M. A. Zwijnenburg, D. J. Adams, A. I. Cooper, *Angew. Chem., Int. Ed.* **2016**, *55*, 1824-1828; eJ. S. Zhang, Y. Chen, X. C. Wang, *Energy Environ. Sci.* **2015**, *8*, 3092-3108.

[2]   X. Wang, K. Maeda, A. Thomas, K. Takanabe, G. Xin, J. M. Carlsson, K. Domen, M. Antonietti, *Nat. Mater.* **2009**, *8*, 76-80.

[3]   A. Thomas, A. Fischer, F. Goettmann, M. Antonietti, J.-O. Muller, R. Schlogl, J. M. Carlsson, *J. Mater. Chem.* **2008**, *18*, 4893-4908.

[4]   F. Goettmann, A. Thomas, M. Antonietti, *Angew. Chem., Int. Ed.* **2007**, *46*, 2717-2720.

[5]   M. J. Bojdys, *Macromol. Chem. Phys.* **2016**, *217*, 232-241.

[6]   aA. P. Cote, A. I. Benin, N. W. Ockwig, M. O'Keeffe, A. J. Matzger, O. M. Yaghi, *Science* **2005**, *310*, 1166-1170; bH. M. El-Kaderi, J. R. Hunt, J. L. Mendoza-Cortes, A. P. Cote, R. E. Taylor, M. O'Keeffe, O. M. Yaghi, *Science* **2007**, *316*, 268-272.

[7]   aA. I. Cooper, *Adv. Mater.* **2009**, *21*, 1291-1295; bJ. X. Jiang, F. Su, A. Trewin, C. D. Wood, H. Niu, J. T. A. Jones, Y. Z. Khimyak, A. I. Cooper, *J. Am. Chem. Soc.* **2008**, *130*, 7710-7720; cY. H. Xu, S. B. Jin, H. Xu, A. Nagai, D. L. Jiang, *Chem. Soc. Rev.* **2013**, *42*, 8012-8031.

[8]   V. R. Thalladi, S. Brasselet, H.-C. Weiss, D. Bläser, A. K. Katz, H. L. Carrell, R. Boese, J. Zyss, A. Nangia, G. R. Desiraju, *J. Am. Chem. Soc.* **1998**, *120*, 2563-2577.

[9]   aI. Nenner, G. J. Schulz, *J. Chem. Phys.* **1975**, *62*, 1747-1758; bR. Fink, C. Frenz, M. Thelakkat, H.-W. Schmidt, *Macromolecules* **1997**, *30*, 8177-8181; cH. Meier, E. Karpuk, H. Christof Holst, *Eur. J. Org. Chem.* **2006**, *2006*, 2609-2617; dS. Ren, Q. Fang, F. Yu, D. Bu, *J. Polym. Sci., Part A: Polym. Chem.* **2005**, *43*, 6554-6561; eT. Yamamoto, S. Watanabe, H. Fukumoto, M. Sato, T. Tanaka, *Macromol. Rapid Commun.* **2006**, *27*, 317-321; fS. Ren, D. Zeng, H. Zhong, Y. Wang, S. Qian, Q. Fang, *J. Phys. Chem. B* **2010**, *114*, 10374-10383; gL. Zou, Y. Fu, X. Yan, X. Chen, J. Qin, *J. Polym. Sci., Part A: Polym. Chem.* **2008**, *46*, 702-712; hK. M. Omer, S.-Y. Ku, Y.-C. Chen, K.-T. Wong, A. J. Bard, *J. Am. Chem. Soc.* **2010**, *132*, 10944-10952; iR. Kannan, G. S. He, T.-C. Lin, P. N. Prasad, R. A. Vaia, L.-S. Tan, *Chem. Mater.* **2004**, *16*, 185-194; jL. Zou, Y. Liu, N. Ma, E. Macoas, J. M. G. Martinho, M. Pettersson, X. Chen, J. Qin, *Phys. Chem. Chem. Phys.* **2011**, *13*, 8838-8846; kL. Zou, Z. Liu, X. Yan, Y. Liu, Y. Fu, J. Liu, Z. Huang, X. Chen, J. Qin, *Eur. J. Org. Chem.* **2009**, *2009*, 5587-5593.

[10]   D. Schwarz, Y. Noda, J. Klouda, K. Schwarzová-Pecková, J. Tarábek, J. Rybáček, J. Janoušek, F. Simon, M. V. Opanasenko, J. Čejka, A. Acharjya, J. Schmidt, S. Selve, V. Reiter-Scherer, N. Severin, J. P. Rabe, P. Ecorchard, J. He, M. Polozij, P. Nachtigall, M. J. Bojdys, *Adv. Mater.* **2017**, *29*, 1703399-n/a.

[11]   S. Ren, M. J. Bojdys, R. Dawson, A. Laybourn, Y. Z. Khimyak, D. J. Adams, A. I. Cooper, *Adv. Mater.* **2012**, *24*, 2357-2361.

[12]   L. Wang, J. Yan, P. H. Li, M. Wang, C. N. Su, *J. Chem. Res.* **2005**, 112-115.

[13]   aI. J. S. Fairlamb, P. S. Bauerlein, L. R. Marrison, J. M. Dickinson, *Chem. Commun.* **2003**, 632-633; bA. S. Batsanov, J. C. Collings, I. J. S. Fairlamb, J. P. Holland, J. A. K. Howard, Z. Lin, T. B. Marder, A. C. Parsons, R. M. Ward, J. Zhu, *J. Org. Chem.* **2005**, *70*, 703-706; cJ.-X. Jiang, F. Su, H. Niu, C. D. Wood, N. L. Campbell, Y. Z. Khimyak, A. I. Cooper, *Chem. Commun.* **2008**, 486-488.

[14]   aQ. Chen, X.-H. Fan, L.-P. Zhang, L.-M. Yang, *Synth. Commun.* **2015**, *45*, 824-830; bS. Wang, D. Hu, W. Hua, J. Gu, Q. Zhang, X. Jia, K. Xi, *RSC Adv.* **2015**, *5*, 53935-53939.

[15]   V. G. Manecke, D. Wöhrle, *Die Makromolekulare Chemie* **1968**, *120*, 176-191.

[16]   D. Tan, W. Xiong, H. Sun, Z. Zhang, W. Ma, C. Meng, W. Fan, A. Li, *Microporous Mesoporous Mater.* **2013**, *176*, 25-30.

[17]   aJ.-X. Jiang, F. Su, A. Trewin, C. D. Wood, N. L. Campbell, H. Niu, C. Dickinson, A. Y. Ganin, M. J. Rosseinsky, Y. Z. Khimyak, A. I. Cooper, *Angew. Chem., Int. Ed.* **2007**, *46*, 8574-8578; bM. Trunk, A. Herrmann, H. Bildirir, A. Yassin, J. Schmidt, A. Thomas, *Chem. - Eur. J.* **2016**, *22*, 7179-7183.

[18]   Y. Liao, J. Weber, C. F. J. Faul, *Chem. Commun.* **2014**, *50*, 8002-8005.

[19]   G. Algara-Siller, N. Severin, S. Y. Chong, T. Björkman, R. G. Palgrave, A. Laybourn, M. Antonietti, Y. Z. Khimyak, A. V. Krasheninnikov, J. P. Rabe, U. Kaiser, A. I. Cooper, A. Thomas, M. J. Bojdys, *Angew. Chem., Int. Ed.* **2014**, *53*, 7450-7455.

[20]   C. Merschjann, T. Tyborski, S. Orthmann, F. Yang, K. Schwarzburg, M. Lublow, M. C. Lux-Steiner, T. Schedel-Niedrig, *Phys. Rev. B* **2013**, *87*, 205204.

[21]   F. K. Kessler, Y. Zheng, D. Schwarz, C. Merschjann, W. Schnick, X. Wang, M. J. Bojdys, *Nat. Rev. Mater.* **2017**, *2*, 17030.

[22]   aY. Yuan, J. Shu, P. Liu, Y. Zhang, Y. Duan, J. Zhang, *J. Phys. Chem. B* **2015**, *119*, 8446-8456; bC. B. Meier, R. S. Sprick, A. Monti, P. Guiglion, J.-S. M. Lee, M. A. Zwijnenburg, A. I. Cooper, *Polymer* **2017**, *126*, 283-290.

[23]   K. D. Gourley, C. P. Lillya, J. R. Reynolds, J. C. W. Chien, *Macromolecules* **1984**, *17*, 1025-1033.

[24]   D. L. Meyer, R. Matsidik, M. Sommer, T. Biskup, *Advanced Electronic Materials*, n/a-n/a.

[25]   S. Kuecken, A. Acharjya, L. Zhi, M. Schwarze, R. Schomacker, A. Thomas, *Chem. Commun.* **2017**, *53*, 5854-5857.

[26]   J. Kiwi, M. Grätzel, *Nature* **1979**, *281*, 657.

COMMUNICATION

Triazine-based graphdiyene polymers are obtained as crystalline and amorphous polymorphs. These polymers are indirect band gap semiconductors with permanent porosity and, hence, interesting as photocatalysts. The crystalline polymorph features efficient charge carrier mobility thanks to an ordered π-aromatic backbone. The amorphous polymorph confines charge carriers locally and is highly fluorescent.

Dana Schwarz, Amitava Acharjya, Arun Ichangi, Yaroslav S. Kochergin, Pengbo Lyu, Maksym V. Opanasenko, Ján Tarábek, Jana Vacek Chocholoušová, Jaroslav Vacek, Johannes Schmidt, Jiří Čejka, Petr Nachtigall, Arne Thomas, Michael J. Bojdys*

Page No. – Page No.

Tuning the porosity and photocatalytic performance of triazine-based graphdiyene polymers *via* polymorphism